Effects of Wave-Current Interactions on the Performance of Tidal Stream Turbines

Stephanie Ordonez-Sanchez[#1], Kate Porter[#2], Carwyn Frost[*1], Matthew Allmark[*2], Cameron Johnstone[#3], Tim O'Doherty[*3]

[#]*Energy Systems Research Unit, University of Strathclyde*
Glasgow, G1 1XJ, United Kingdom
[1]s.ordonez@strath.ac.uk
[2]kate.porter@strath.ac.uk
[3]cameron.johnstone@strath.ac.uk
[*] *School of Engineering, Cardiff University*
Cardiff CF24 3AA, United Kingdom
[1] frostc1@cardiff.ac.uk
[2]AllmarkMJ1@cardiff.ac.uk
[3]Odoherty@cardiff.ac.uk

Abstract—**The main objective of this paper is to analyse extreme cases of wave-current interactions on tidal stream energy converters. Experiments were undertaken in the INSEAN tow tank facility where flow velocities of 0.5 and 1m/s were used with and without waves. The wave variations studied in this testing campaign were between wave heights of 0.2 to 0.4m with a 2s wave period. These wave conditions were considered extreme cases considering the use of a turbine with a rotor diameter of 0.5m. The turbine was equipped with a torque transducer, an encoder and a strain gauge to measure power coefficients and forces on a single blade root. Therefore, the results of this experiment are used to improve the understanding of wave effects on tidal stream rotors by analysing not only the temporal variations of power and blade loading but also the peak variations of them.**

Keywords— **Tidal Turbine, Extreme Environment, Wave-Current Interactions, Experiments.**

I. INTRODUCTION

The development of marine energy technology has increased rapidly in recent years. However, the industry has not yet reached a stage of commercial viability, and to date, only single turbine prototypes have been tested in the field ([6]). One reason for the difficulty in achieving financial viability in the industry is the complex and often extreme nature of the loading conditions seen by turbines that result from unsteadiness in the flow. The majority of projects have been deployed in areas no deeper than 40m which means that full-scale turbines operate in areas between 3-5D, assuming a turbine rotor diameter (D) between 10-20m. Depending on the site, the geometry of the turbine and type of support structure used (e.g. floating or rigid foundation) the turbine rotors will be affected partially or fully by wave-current interactions. For example, at one tidal energy site the penetration of waves typically reaches as much as 1/3rd of the water column ([8]).

The computational study of Tatum, et al. (2015) [9] indicated that the variation of bending moments on the blades due to the oscillatory motion of waves will translate into forces directly applied to small areas of the drivetrain, which will affect components such as bearings and seals. Nevalainen, et al. (2015) [7] also showed numerically that the turbine shaft is highly affected by wave motion. Thus, the sinusoidal variations in wave-current velocities have the potential to reduce significantly the life of the drivetrain components and the rotor blades.

A number of experimental studies investigating the effects of wave-current interaction on turbines can be found in [1,3-5]. (Barltrop, et al., 2007) [1] undertook a large number of tests with a horizontal axis turbine type (HAT) of 0.4m rotor diameter in a tow tank. In their work, information related to wave-current interactions on a tidal turbine in varying flow velocity, wave frequency and wave height for medium-high wave environments was presented. Their work gave a good insight and initial analysis on this matter. However, the results presented in this work were only obtained for one small fraction of the power and thrust curves and thus the effects of waves and currents are not fully visualised.

Similarly to [1], (Gaurier, et al., 2013) [4] carried out experiments to study wave-current interaction in a flume tank by varying the period and frequency of waves. Although the investigations done in [4] gave a very good understanding of wave-current interactions by studying three waveforms with two different wave heights and two different wave frequencies, the mean current velocity was similar in all the cases, and thus it is not possible to identify the effects of current and waveform variation.

More recently, Henriques, et al., 2014 [5] undertook experimental analysis in a flume tank using a single flow speed of 0.5 m/s and a turbine of 0.5m rotor diameter. They found small differences between power and thrust coefficients when comparing the wave-current and exclusively current

experiments, as previously seen in [1] and [4]. However, they undertook their analysis in a small flume tank with a blockage factor of almost 37%. This magnitude, which is related to the ratio of the swept area of the rotor to the cross sectional area of the corresponding test facility, can have significant effects on the performance of the turbines as has been studied by Consul, et al., 2013 [2]. Galloway, et al., 2014 [3] also investigated wave-current interactions on marine turbines; but in this case, the experimental campaign was only focused on a single wave-current event.

It can be seen that in most of the experiments the wave heights and periods are related to medium-high wave climates. Also, the wave-current interactions are usually done for a single flow speed or a similar variation of it. Therefore, this investigation provides information on the effects of extreme conditions of wave-current interactions on a tidal turbine at two different flow velocities while working in low blockage ratio conditions.

II. Experimental Set-Up

A scaled horizontal axis turbine of 0.5m in diameter was utilised in this testing campaign. The rotor was composed of three Wortmann FX 63-37 blade profiles. The tests were carried out at the 3.5 x 9 x 220m CNR-INSEAN towing tank facility. Two flow regimes of 0.5 and 1.0 m/s were set during the experiments, with variations of wave height of 0.2 to 0.4 m and a period of 2 s. Table I describes the waveforms used during the experiments.

TABLE I
WAVES PARAMETERS UTILISED IN THE EXPERIMENTS

Waveform	Wave height (m)	Wave Period (s)
WF1	0.4	2
WF2	0.3	2
WF3	0.2	2

The turbine hub centre was installed 1m below the water level with the use of a steel pole, attached directly to the towing carriage. The thickness of the steel pole was chosen to prevent significant vibrations occurring while the turbine was in operation. Figure 1 shows the turbine installed in the facility.

Measurements of torque and angular velocities were obtained using the motor controller of the system. Additionally, the turbine was equipped with a custom built strain gauging system to measure the forces at the root of one of the blades. A wave probe to measure the accuracy of the wave height created by the wave makers was also installed on the carriage along with a pitot tube to measure the flow velocity at which the turbine was operating. A National Instruments data acquisition system was used during the experiments. The data was sampled at 250Hz.

Fig. 1: Turbine set-up in the CNR-INSEAN tow tank.

III. Methodology

A comparative analysis of the performance characteristics of the turbine is presented in this paper as C_p-TSR curves comparing the power capture under wave and no wave conditions. The power coefficient (C_p) was calculated as:

$$C_p = P/0.5\rho A V^3$$

where P is the calculated average power generated. In this case it is calculated from the torque generating current (TGC) and the rotational speed (Ω). The methodology for obtaining the rotor torque from the motor TGC is presented in Section A. *A* is the swept area of the rotor, and V denotes the unidirectional flow velocity, in this case the tow tank carriage velocity. The density of the water used to calculate C_p was 992 kg/m^3.

The average C_p is plotted against the average TSR values for each time series, where TSR denotes the ratio between the blade tip speed and the flow velocity (V):

$$TSR = \Omega r/V$$

r represents the radius of the rotor and Ω is the angular velocity of the turbine.

The average blade root force measurements are plotted against TSR without non-dimensionalising the data. The reason behind this is that force measurements was only taken for a single blade. Thus, the thrust coefficient cannot be determined for the full rotor due to the wave effects preventing the forces on one blade being equal to those on the other two. It was determined that multiplying the forces by three would not be the thrust developed by the rotor. Nevertheless, studying the blade root forces for one blade can provide useful insights into the wave-current effects, especially when considering the structural performance and fatigue life of a turbine blade.

A. Torque Generating Current

A motor calibration to measure the frictional torque developed by the motor over a range of rotational velocities was undertaken. The results are shown in Figure 2. The frictional torque was obtained by measuring the torque generating current in a water basin without the tidal rotor blades. Various points at different rotational speeds were obtained and thus, a square polynomial approximation was calculated. This approximation was then used to determine the proportion of the measured torque during the experiments that could be attributed to the turbine rotor.

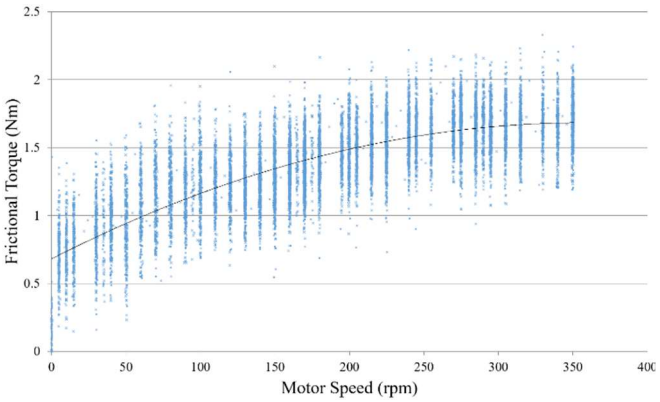

Fig. 2 Frictional torque obtained at various rotational speeds in stationary conditions.

B. Blade Root Forces

The blade force was calibrated by fitting several calibration weights in close proximity to the blade root connection. A linear trendline was obtained for this calibration and was used to process the raw data of the strain gauge.

An initial measurement of the blade force was obtained immediately prior to each experiment during stationary conditions; i.e. carriage at rest. This value was then subtracted from the recorded blade force value in order to convert the raw signal into informative data of the blade forces.

IV. Results and Discussion

The performance characteristics of the turbine presented in this result section include the average C_p-TSR curves for each carriage speed and the average blade root forces plotted against average TSR. The temporal variations of torque were also investigated when varying the wave height in the experiments. This information is complemented with a frequency domain analysis.

To improve understanding of the impact that the blade position in the water column relative to the wave phase has on loading, the time series of the blade root force measurements are considered and the peak forces occurring in the blade root are also quantified in the following sections.

However, before these results are presented, the measurements of wave height and flow velocity are first discussed.

A. Wave and Flow Speed Measurements

The quality of the waveforms was checked using a wave probe installed in the towing carriage. During this paper, the results using two flow speeds and an extreme waveform with a height of 0.4m were mostly investigated. However, two additional wave heights were investigated and thus quality of the waveform was verified for each case. A summary of the mean wave heights and periods for some of the tests is depicted in Tables III and IV.

TABLE III
Wave Height Measurement at a Flow Speed of 0.5 m/s

Cases	WF1	WF2	WF3
Mean Wave Height (m)	0.41	0.30	0.20
Mean Wave Period (s)	1.73	1.72	1.72
Standard deviation Wave Height (m)	0.02	0.01	0.01
Standard deviation Wave Period (s)	0.04	0.04	0.03

TABLE IV
Wave Height Measurement at a Flow Speed of 1 m/s

Cases	WF1	WF2	WF3
Mean Wave Height (m)	0.37	0.29	0.19
Mean Wave Period (s)	1.52	1.51	1.51
Standard deviation Wave Height (m)	0.02	0.01	0.01
Standard deviation Wave Period (s)	0.04	0.04	0.08

Figure 3(a) and (b) show the typical measured water surface elevation for each of the tow speeds used in these experiments with WF1. The wave height varies by a small amount compared to the design value, probably due to limitations in the wavemaker control system which does not have active absorption capabilities. The wave period in the signal is in agreement with that expected from superposition of the steady current value, based on a design period of 2 s with a stationary carriage. The distance from still water level to the crest is a little larger than the distance from the still water level to the trough so that the wave form contains some non-linearity. This indicates that higher order wave theory should be used to accurately model the waves. The smallest wave height gives a more linear profile with the wave crest and trough amplitudes more similar to each other. This is in agreement with the expected trend of wave non-linearity increasing with wave steepness.

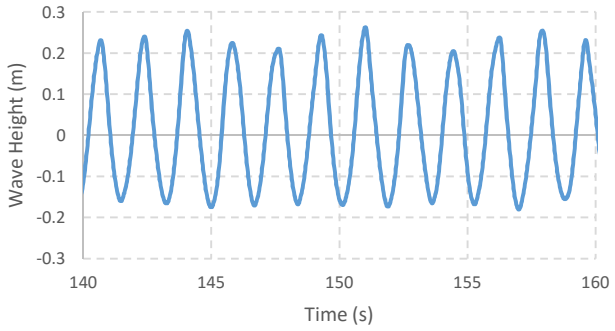

(a)

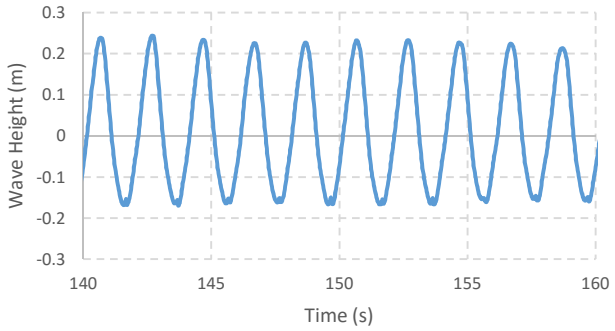

(b)

Fig. 3 Typical wave surface elevation at a) 0.5m/s and b)1 m/s with the largest of the three wave heights tested.

The flow measurements were undertaken using a Pitot tube. The calibration method for the Pitot tube was determined to be equal to the theoretical Pitot equation with no additional correction factors. This approach gives a reasonably good agreement between the independent carriage velocity measurement and that from the Pitot tube for the steady current tests. A representative measurement of the flow velocity in waves is observed in Figure 4 using a carriage velocity of 1m/s. This shows reasonable agreement with the superimposed current and wave velocities computed from linear wave theory.

B. Power Results

Figure 5 shows the results of the experiments undertaken at 0.5 and 1m/s using only WF1. It can be seen that similarly to the literature, the average C_p of the turbine when working under wave-current conditions is similar to that of a turbine operating in uniform current.

The standard deviation results, shown in Figure 3, are higher by >50% compared to those found in the literature (e.g. [4]) which informs the effects of extreme wave-current interactions on the power generation of the turbines under such conditions. As the TSR increases, the standard deviation or variation in the C_p increases. It can be observed that this is higher for the 0.5m/s case where the wave velocity is equal to a greater proportion of the current velocity.

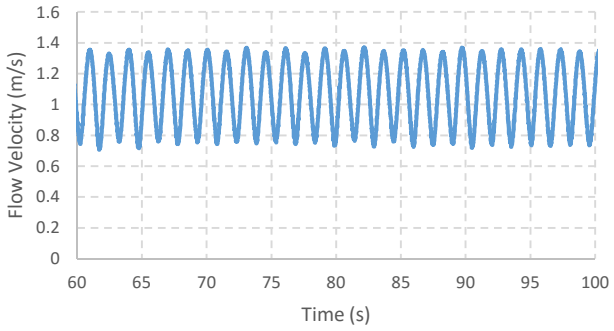

Fig. 4 Flow speed measured with a Pitot tube at 1m/s carriage speed with regular WF1

It is worth mentioning that the control technique used in the experiments is a speed control, similar to that used in [4]. In order to carry out initial investigations of using a different control technique, a torque control case was investigated. The results can be observed in Figures 5(b) and 6(b) highlighted in green. It can be seen that the C_p values follow the same pattern as those produced using speed control techniques. Of course, the variations of torque are minimal, and this result is comparable to the information presented in [5]. However, further investigations on this matter are required to confirm the full extent of the resemblances with the previously mentioned author.

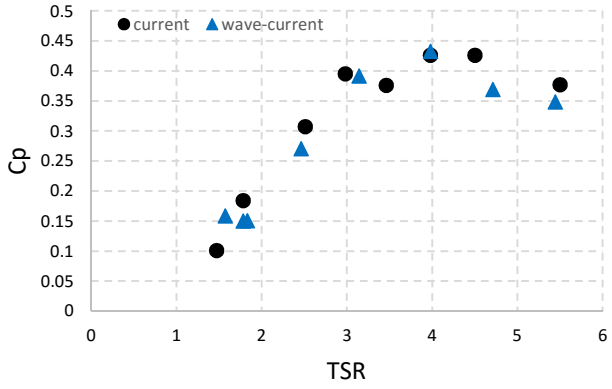

(a)

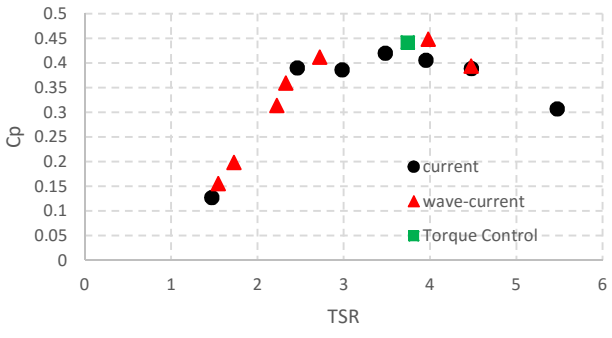

(b)

Fig. 5 Power coefficient of the turbine working during extreme wave-current events (red and blue) and during current alone (black) at a) 0.5m/s and b)1 m/s.

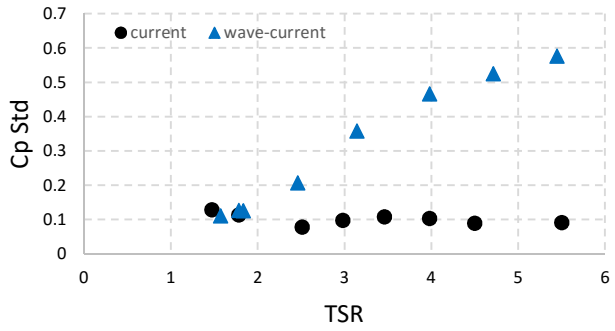

(a)

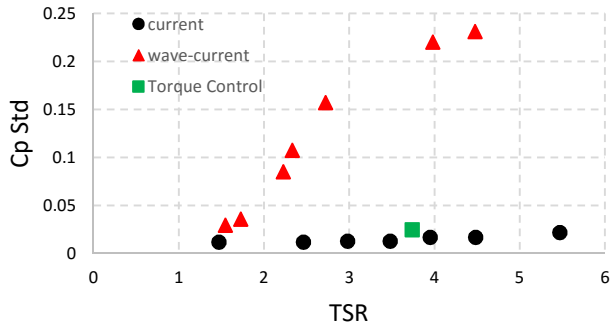

(b)

Fig. 6 Standard deviation of the power coefficient of the turbine working during extreme wave-current events (red and blue) and during current alone (black) at a) 0.5m/s and b)1 m/s.

C. *Wave Height Variation – Time Domain Analysis*

To investigate the effects of different wave parameters on the torque, two additional experiments were undertaken at three operating TSR points and two different flow velocities. These are summarised in Table V.

TABLE V
CASES STUDIED USING VARIATIONS OF WAVEFORMS

Cases	Flow Velocity (m/s)	TSR	Waveform
1	0.5	2.5	WF1,WF2,WF3
2	0.5	3.5	WF1,WF2,WF3
3	1	3.5	WF2,WF3

The following Table VI gives a summary of the mean power coefficient calculated for each of the waveform cases. The averaged C_p for each of the cases is similar with a slight discrepancy <5%. The major inconsistency is observed between WF1 and WF2 of Case 2. As expected, the variation of the C_p which in this case is given by the standard deviation decreases with a similar magnitude as the wave height decreases.

TABLE VI
MEAN AND STANDARD DEVIATION OF THE POWER COEFFICIENT FOR EACH WAVEFORM CASE

Cases	WF1	WF2	WF3
Case 1	0.27±0.21	0.26±0.17	0.27±0.20
Case 2	0.44±0.40	0.35±0.31	0.32±0.22
Case 3	-	0.43±0.15	0.44±0.11

When analysing the torque variations, it can be observed in Figure 7 that the torque fluctuations decrease as the wave height drops. It is noticeable that the highest peak fluctuations are obtained for Case 3 when comparing the three cases showing the influence of the tow speed velocity. This is especially significant since these parameters will need to be considered when fatigue analysis is carried out on the components of the drivetrain, as observed in [7].

The torque presented in Figure 7 has less fluctuations about the mean compared to the existent literature (e.g. [4]). However, the reason may be the absence of turbulent flow which was identified in other experiments presented in the existent literature.

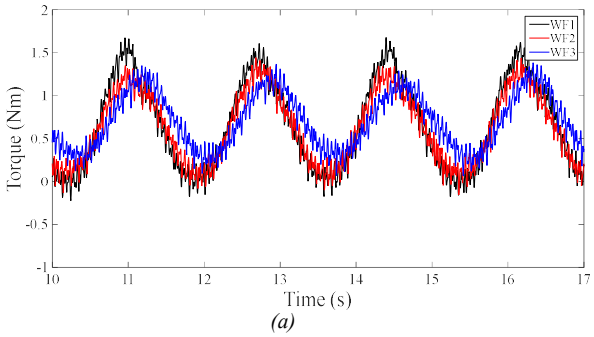

(a)

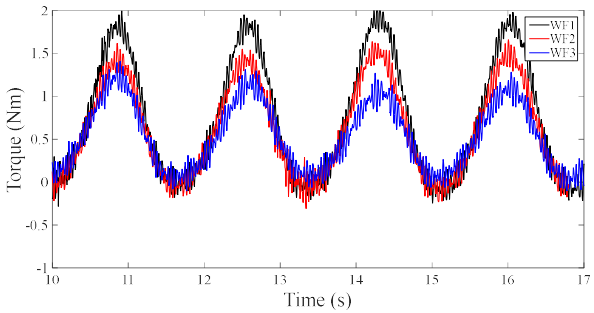

(b)

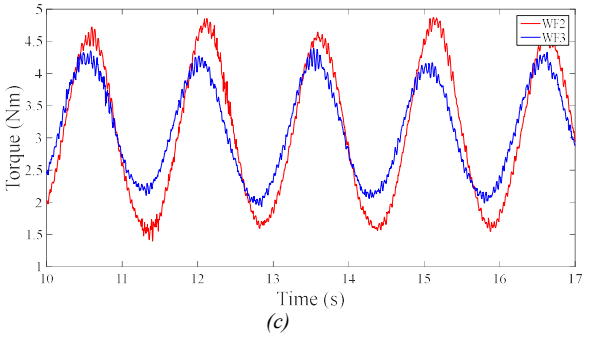

(c)

Fig. 7 Torque variation for three different wave forms when the turbine was operating at: a) 0.5m/s and TSR=2.5, b) 0.5m/s and TSR=3.5 and c) 1m/s and TSR =3.5

D. Wave Height Variation – Frequency Domain Analysis

The torque signals were also analysed in the frequency domain using FFT analysis. Figure 8 presents the characteristic patterns obtained in the frequency domain analysis undertaken in the torque signals. It can be seen that the main frequency is that of the wave period followed by the rotational frequency of each of the cases, 0.7, 1.1 and 2.2Hz for Case 1, 2 and 3 respectively. The other notable frequencies are related to the supporting pole at 10 and 20 times the rotational frequency. Those frequencies are less evident at flow velocities of 1m/s where the characteristic frequency of the wave period is more defined, opposite to those frequencies obtained in the experiments at 0.5m/s.

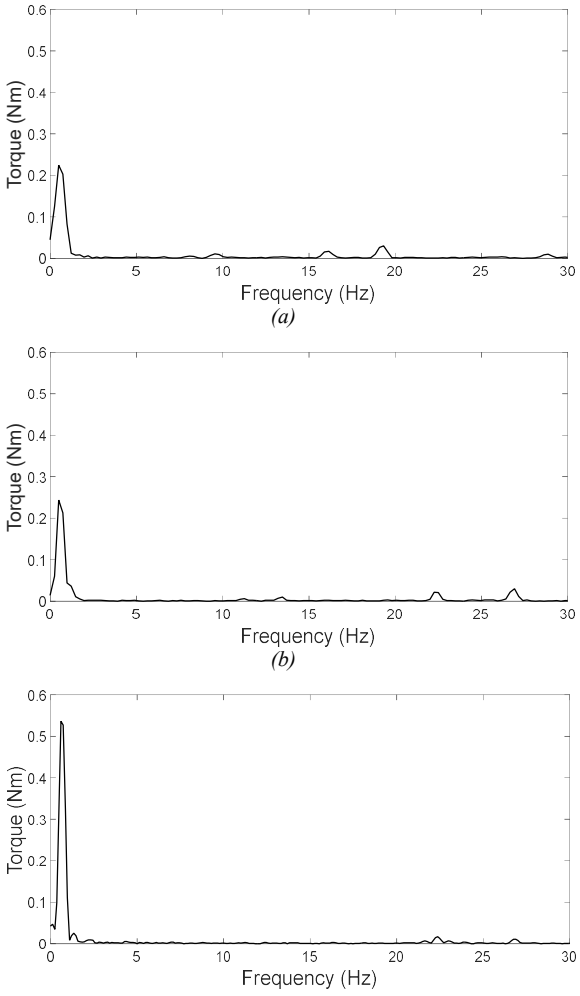

Fig. 8 Frequency domain analysis of torque variation when the turbine operates at: a) 0.5m/s and TSR=2.5, b) 0.5m/s and TSR=3.5 and c) 1m/s and TSR=3.5 using WF3.

E. Blade Root Forces

Figure 9 shows the results obtained for the blade root forces measured on one blade. It can be seen that there is a reasonable match between the average blade root forces measured during the wave-current cases and during the normal operating condition (current alone) at the 0.5m/s carriage speed. However, for the 1m/s carriage speed tests the average forces are a little higher in the wave-current cases compared to under current alone.

The fluctuations in the loads are investigated in Figure 10 where the difference between the maximum and minimum blade forces are plotted against the number of rotor revolutions per wave period for each test. This was done to understand the range of loading that is generated on the blade and the relationship between the wave period and turbine rotational period, at the two different flow speeds. It is observed in Figure 10 that the blade force oscillations are greater at low flow velocities, and increase as the turbine rotational velocity increases compared to the wave period.

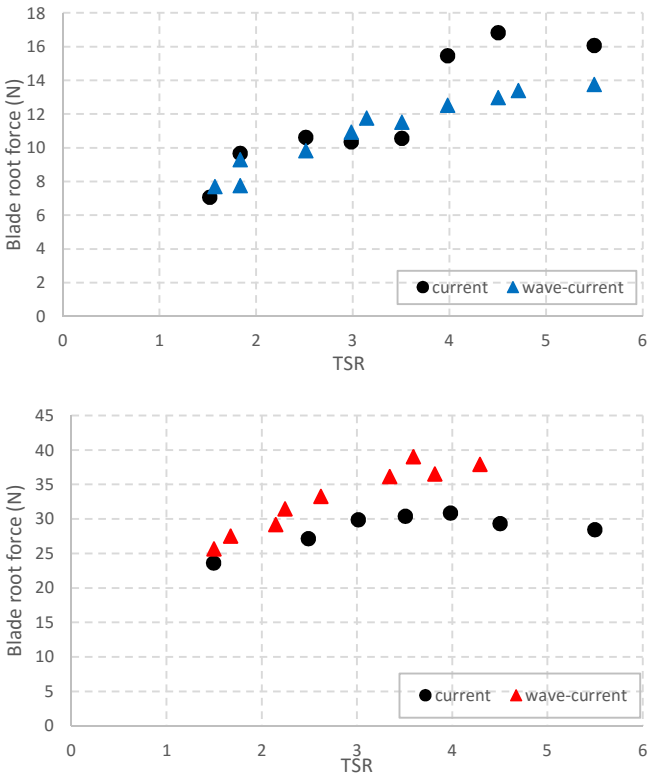

Fig. 9 Average blade forces of a turbine blade working during extreme wave-current events and during normal conditions (current alone) at a) 0.5m/s b) 1 m/s.

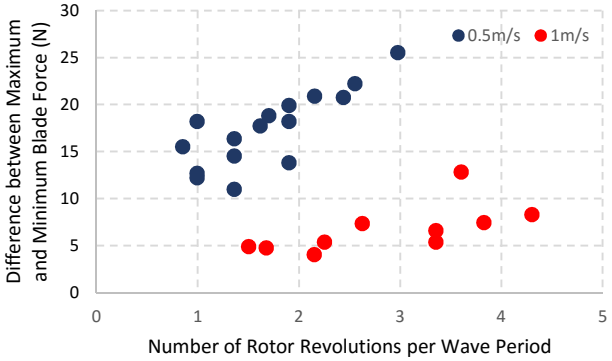

Fig. 10 Difference between maximum and minimum blade forces versus the rotor speed in rpms to the wave period ratio.

F. *Time series of blade forces*

More detail about the blade loading can be obtained from investigating the blade force time series. Figure 9 shows some representative force time signals from the 0.5m/s tests with WF1. What is particularly evident is the significant difference in the pattern of the signal, depending on the rotor speed. The difference in the time series patterns is important because it may have a significant effect on the fatigue life of the blade.

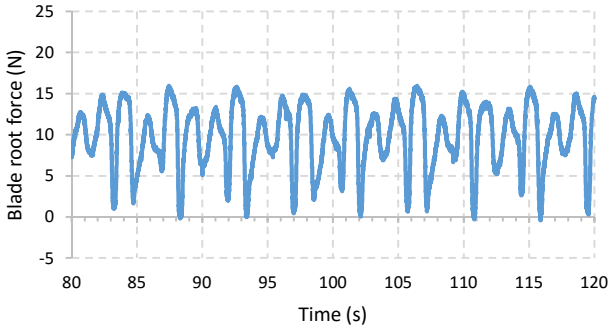

(a)

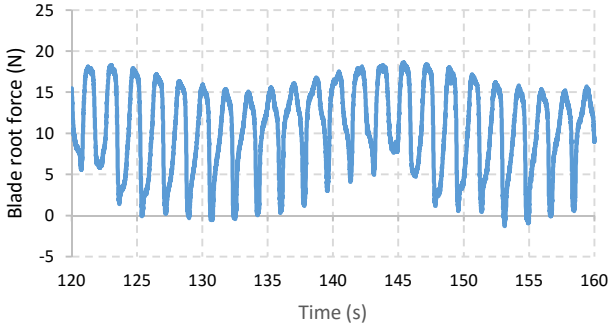

(b)

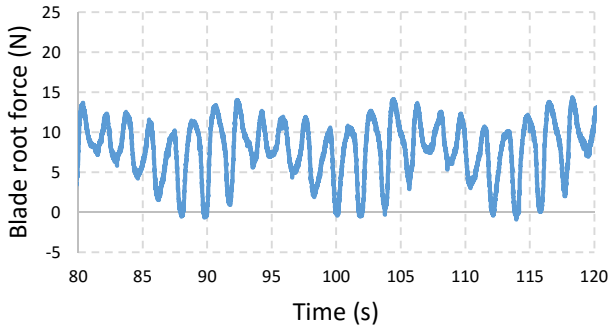

(c)

Fig. 11. Time series of the blade forces at three different rotor speeds: a) TSR=2.5, b) TSR=3.5 and c) TSR=1.6. Each of them measured during the experiments when the carriage was operated at 0.5m/s, WF1.

Figure 12 shows a characteristic time series from a test at 1m/s carriage speed with WF1. The loading patterns are more regular at this carriage speed, indicating that the magnitude of the wave compared to the current velocity has a significant influence on the loads on the turbine.

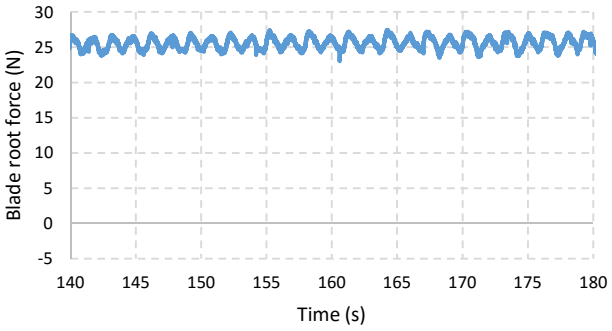

Fig. 12. Time serie of the blade forces at TSR=1.6 measured during the experiments when the carriage was operated at 1m/s, WF1.

G. *Time series of blade forces during wave crest and trough*

Two more experiments were carried out to evaluate the blade forces when either the wave crest or trough coincided with the instrumented blade passing the upright position. Figure 13 shows the time series of the strain gauge signal for the two cases synchronised with the wave crest and trough respectively.

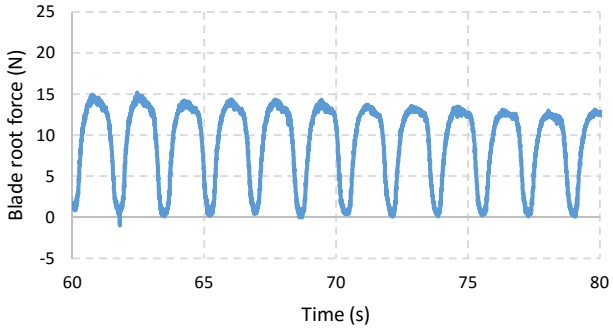

(a)

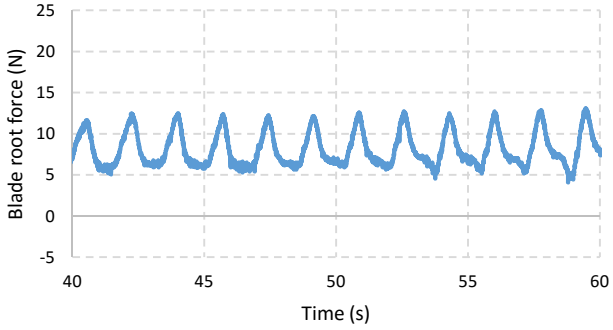

(b)

Fig. 13 Blade forces when the upright blade synchronised with: a) a wave crest passing and b) a wave trough passing at a carriage speed of 0.5m/s. In both cases the turbine is operating at a TSR=1.8.

In these signals the fluctuations are more regular, as the turbine rotational speed was set equal to the apparent wave period, although there is some change in the force pattern with time due to the approximate nature of the synchronisation which for this preliminary pair of tests was done by eye. The loading fluctuations are noticeably reduced in the test where

the wave trough coincides with the upright blade. This indicates that over short time periods the magnitude of the load fluctuations is highly dependent on the relationship between the phase of the wave and the blade position in the water column.

V. Conclusions

A comparative analysis of the performance characteristics of a turbine operating under extreme wave-current conditions is presented in this paper. It was found that the average power matched that under current alone, but the standard deviation was substantially higher that the information presented in the existent literature. Furthermore, the standard deviation increased with the tip speed ratio, indicating a strong dependence on the relationship between the wave period and the turbine rotational speed.

Two additional cases were tested where the wave heights were reduced, which resulted in similar power coefficients but a reduction in power coefficient variation. It was also observed through a frequency domain analysis that external effects such as the supporting structure can have certain effects on the torque measurements.

An evaluation of blade forces on one of the turbine blades show the different force patterns generated when the angular velocity of the turbine changes. Severe oscillations of forces on turbine blades can lead to a reduced lifespan of the blades which are expensive components of the tidal turbines.

VI. Acknowledgments

The authors would like to thank the staff members at INSEAN for their assistance during testing. and also would like to acknowledge the MaRINET Transnational Access Program for funding this work.

References

1. Barltrop, N. et al., 2007. Investigation into wave-current interactions in marine current turbines,. *Proc. IMechE Vol. 221 Part A: J. Power and Energy.*.
2. Consul, C. A., Willden, R. H. J. & McIntosh, S. C., 2013. Blockage effects on the hydrodynamic performance of a marine cross-flow turbine. *Philosophical Transactions of the Royal Society A.*
3. Galloway, P., Myers, L. & Bahaj, A., 2014. Quantifying wave and yaw effects on a scale tidal stream turbine. *Renewable Energy, 63,* pp. 297-307.
4. Gaurier, B., Davies, P., Deuff, A. & Germain, G., 2013. Flume tank characterization of marine current turbine blade behaviour under current and wave loading. *Renewable Energy, 39,* pp. 1-12.
5. Henriques, T. d. J. et al., 2014. The effects of wave–current interaction on the performance of a model horizontal axis tidal turbine. *International Journal of Marine Energy, 8 ,* pp. 17-35.
6. Mofor, L., Goldsmith, J. & Jones, F., 2014. *Ocean Energy: Technology readiness, Patents, Deployment Status and Outlook.,* s.l.: International Renewable Energy Agency (IRENA).
7. Nevalainen, T., Johnstone, C. & Grant, A., 2016. A sensitivity analysis on tidal stream turbine loads caused by operational, geometric design and inflow parameters. *International Journal of Marine Energy ,* Volume 16, pp. 51-64.
8. Norris, J., & Droniou, E. (2007). Update on EMEC activities, resource description, and characterisation of wave-induced velocities in a tidal flow. European Wave and Tidal Energy Conference (EWTEC) . Porto, Portugal: EWTEC.
9. Tatum, S. et al., 2015. Wave–current interaction effects on tidal stream turbine performance and loading characteristics.. *International Journal of Marine Energy. ,* pp. 161-179.